

# Natural Convection from a Permeable Sphere Embedded in a Variable Porosity Porous Medium Due to Thermal Dispersion

S. M. M. EL-Kabeir, M. A. El-Hakiem, A. M. Rashad

Department of Mathematics, Faculty of Science  
South Valley University  
Aswan, Egypt  
am\_rashad@yahoo.com

**Received:** 08.10.2006 **Revised:** 21.02.2007 **Published online:** 31.08.2007

**Abstract.** The laminar natural convection boundary-layer flow of an electrically-conducting fluid from a permeable sphere embedded in a porous medium with variable porosity is considered. The non-Darcy effects including convective, boundary, inertial and thermal dispersion effects are included in this analysis. The sphere surface is maintained at a constant heat flux and is permeable to allow for possible fluid wall suction or blowing. The resulting governing equations are nondimensionalized and transformed into a nonsimilar form and then solved numerically by using the second-level local non-similarity method that is used to convert the non-similar equations into a system of ordinary differential equations. Comparisons with previously published work are performed and excellent agreement is obtained. A parametric study of the physical parameters is conducted and a representative set of numerical results for the velocity and temperature profiles as well as the local skin-friction coefficient and the Nusselt number are illustrated graphically to show interesting features of Darcy number, inertia coefficient, the magnetic parameter, dimensionless coordinate, dispersion parameter, the Prandtl number and suction/blowing parameter.

**Keywords:** porous medium, natural convection, non-Darcy, Forchheimer number, thermal dispersion, sphere.

## 1 Introduction

Convective heat transfer from fixed or rotating bodies in a porous media represents a problem that can be related to numerous engineering applications. This occurs both naturally in the geophysical environment through the flow of water in porous rocks and in many engineering and technological systems. Such problems are of great practical interest, for example, in the geothermal recovery of heated water, prevention of sub-soil water pollution, insulation systems, heat exchangers, building thermal insulation, enhanced oil recovery, nuclear waste disposal, metal casting, grain storage, and heat

transfer in electronic equipment, among many others. The problem of mixed, forced, and free convection about a solid sphere in a viscous incompressible fluid has received relatively little attention. To the best knowledge of the authors, the only such studies which have been reported are the experimental work of Yuge [1] and Klaychko [2], and the analytical work of Hieber and Gebhart [3]. These studies, both experimental and analytical, were conducted under the action of very small Reynolds and Grashof numbers. Chen and Mucoglu [4, 5] have later studied mixed convection over a sphere with uniform surface temperature and uniform surface heat flux. Chiang et al. [6] reported an exact analysis of laminar free convection over a sphere for the cases of uniform wall temperature and uniform heat flux. Huang and Chen [7] solved the laminar free-convection flow about a sphere with surface blowing and suction effects, while Lien et al. [8] considered mixed and free convection over a rotating sphere with wall suction and blowing. Yih [9] investigated the viscous dissipation, Joule heating and heat source/sink effects on non-Darcy MHD natural convection flow over an isoflux permeable sphere in uniform porous media. Chamkha and Al-Mudhaf [10] formulated the coupled heat and mass transfer by natural convection from a permeable sphere in the presence of an external magnetic field and thermal radiation effects.

All the above studies neglect thermal dispersion effects. Plumb [11] pointed out that when the inertial effects are prevalent; the thermal dispersion effects in a porous medium become very important. Hong et al. [12] studied natural convection from a non-isothermal vertical wall in a non-uniform porous medium, and thermal dispersion effects are included in the energy equation. The thermal dispersion effect on non-Darcy convection over horizontal and vertical walls has been studied by Lai and Kulacki [13, 14]. Amiri and Vafai [15] confirmed in their study on forced convection flow and heat transfer that the axial dispersion effect may be neglected when compared with the radial dispersion effect. An analysis of thermal dispersion effect on vertical plate natural convection in porous media is presented by Hong and Tien [16]. Effect of thermal dispersion on non-Darcy natural convection over a vertical flat plate and also isothermal vertical cone in a fluid saturated porous medium were studied by Murthy and Singh [17, 18].

Motivated by the investigations mentioned above, the purpose of the present work is to investigate the thermal dispersion effect on non-Darcy MHD natural convection flow over a permeable sphere maintained at uniform heat flux in a variable porosity porous medium.

## 2 Governing equations

Consider the steady natural convection two-dimensional laminar non-Darcy magneto-hydrodynamic natural convection flow over a permeable sphere embedded in a fluid-saturated porous medium having a variable porosity distribution with thermal dispersion effect. A uniform magnetic field is applied in the direction normal to the surface. The surface of the sphere, subject to mass transfer, is maintained at a uniform heat flux  $q_w$ . Constant suction or injection is imposed at the surface of the sphere. The schematics of the problem under consideration and the coordinate system are shown in Fig. 1. The fluid is assumed to Newtonian, incompressible, viscous and electric-conducting. Fluid

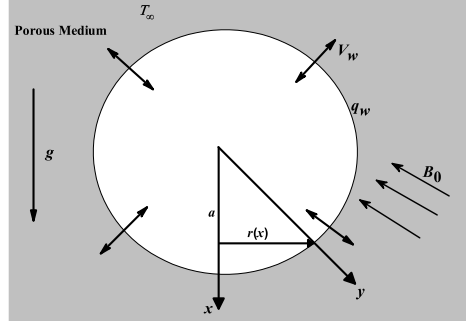


Fig. 1. Flow model and coordinate system.

properties are assumed to be constant except the density variation in the buoyancy force term. A magnetic field of constant strength is applied in the negative  $y$  direction at all times. Its interaction with the electrically conducting working fluid produces a resistive force in the negative  $x$  direction. This force is called the Lorentz force. The magnetic Reynolds number is assumed to be small so that the induced magnetic field is neglected. In addition, no electric field exists and the Hall effect, the magnetic or Joule heating, and viscous dissipation are all neglected. Upon treating the fluid-saturated porous medium as a continuum (see, Vafai and Tien [19]), including the non-Darcian boundary, inertia and variable porosity effects, and assuming that the Boussinesq approximation is valid, the boundary-layer form of the governing equations can be written as (see, Vafai and Tien [19] and Gebhart et al. [20]),

$$\frac{\partial(ru)}{\partial x} + \frac{\partial(rv)}{\partial y} = 0, \quad (1)$$

$$\frac{\rho}{\varepsilon^2} \left( u \frac{\partial u}{\partial x} + v \frac{\partial u}{\partial y} \right) = \frac{\mu}{\varepsilon} \frac{\partial^2 u}{\partial y^2} + g \sin \left( \frac{x}{a} \right) \beta \rho (T - T_\infty) - \sigma B_0^2 u - \frac{\mu}{K(y)} u - \frac{\rho F(y)}{\sqrt{K(y)}} u^2, \quad (2)$$

$$u \frac{\partial T}{\partial x} + v \frac{\partial T}{\partial y} = \frac{\partial}{\partial y} \left( \alpha_y \frac{\partial T}{\partial y} \right). \quad (3)$$

The boundary conditions for this problem are defined as follows:

$$\begin{aligned} y = 0: \quad & u = 0, \quad v = V_w, \quad q_w = -k_e \left( \frac{\partial T}{\partial y} \right). \\ y \rightarrow \infty: \quad & u = 0, \quad T = T_\infty. \end{aligned} \quad (4)$$

Where  $x$  is measured along the surface of sphere from the lower stagnation point and  $y$  is measured normal to the surface, respectively,  $r$  is the radial distance from symmetric axis to surface.  $r = a \sin(x/a)$ , where  $a$  is the radius of the sphere.  $u$  and  $v$  are the velocities in the  $x$ - and  $y$ -directions.  $g$ ,  $\beta$ ,  $\mu$ ,  $\rho$  and  $T$  are the gravitational acceleration, the thermal

expansion coefficient, the fluid dynamic viscosity, the fluid density and the temperature, respectively.  $\sigma$  and  $B_0$  are the electrical conductivity and the externally imposed magnetic field in the  $y$ -direction, respectively.  $K(y)$  and  $F(y)$  are the porous medium permeability and geometric function depends on porosity only, respectively.  $\alpha_y$  is the effective thermal diffusivity in  $y$ -direction, where  $k_e$  is the effective thermal conductivity of the porous medium which is the sum of the molecular conductivity  $k$  and the dispersion thermal conductivity  $k_d$ .  $V_w$  is the uniform surface suction ( $< 0$ ) or blowing ( $> 0$ ) velocity.

The variable porosity model to be supplemented with equations (1) through (3) is the one employed by Poulikakos and Renken [21] in their work on forced convection in porous medium channels and pipes. Furthermore, permeability  $K(y)$  and the geometric function  $F(y)$  are expressed as [15, 22]

$$K(y) = \frac{\varepsilon^3 d^2}{150(1 - \varepsilon)^2}, \tag{5}$$

$$F(y) = \frac{1.75}{\sqrt{150} \varepsilon^{3/2}}, \tag{6}$$

and variable porosity can be expressed as [15, 22]

$$\varepsilon(y) = \varepsilon_\infty \left[ 1 + b \exp\left(-\frac{cy}{d}\right) \right], \tag{7}$$

where  $d$  is the particle diameter,  $\varepsilon$  is the porosity of the porous medium,  $\varepsilon_\infty$  is the porosity near the ambient conditions, and  $b$  and  $c$  are empirical constants that depend on the ratio of the porous bed to particle diameter (Vafai et al. [23]). As mentioned before, the exponential relation between the porosity and the normal distance from the boundary surface is an approximate representation of the experimental data reported by Benenati and Brosilow [24] for their study on void fraction distribution in packed beds. The values of  $\varepsilon_\infty$ ,  $b$ , and  $c$  employed in the present work are 0.5, 0.98, and 1, respectively. These values were found to give a good approximation to the data reported by Benenati and Brosilow [24] for a particle diameter of 4 mm.

Following Murthy and Singh [17, 18], the quantity  $\alpha_y$  is variable and is defined as  $\alpha_y = \alpha + \alpha_d$ , where  $\alpha, \alpha_d = \gamma d|u|$  are the molecular thermal diffusivity, dispersion thermal diffusivity, where  $\gamma$  is the mechanical dispersion coefficient whose value depends on the experiments and  $d$  is the particle diameter. This model for thermal dispersion has been used extensively by researchers like Plumb [11], Hong and Tien [12] and Lai and Kulacki [13] in studies of convective heat transfer in non-Darcy porous media.

It is convenient to transform equations (1)–(4) by using the following nonsimilarity transformations reported earlier by Yih [9] and Chamkha and Al-Mudhaf [10]:

$$\begin{aligned} \xi &= \frac{x}{a}, \quad \eta = \frac{y}{a}(Gr)^{1/5}, \quad \psi = \nu \xi (Gr)^{1/5} f(\xi, \eta), \\ \theta(\xi, \eta) &= \frac{k(Gr)^{1/2}(T - T_\infty)}{aq_w}, \quad Gr = \frac{g\beta q_w a^4}{\nu^2 k}, \quad \nu = \mu/\rho, \end{aligned} \tag{8}$$

where  $Gr$  is the Grashof number,  $\nu$  is the kinematic viscosity, and  $\psi$  is the stream function defined as  $ru = \partial(ru)/\partial y$  and  $rv = -\partial(rv)/\partial x$ , therefore the continuity equation is

identically satisfied. In addition the velocities components are

$$u = \frac{\nu(Gr)^{2/5}}{a} \xi f', \quad v = -\frac{\nu(Gr)^{1/5}}{a} \left[ \xi \frac{\partial f}{\partial \xi} + \left( 1 + \frac{\xi \cos \xi}{\sin \xi} \right) f \right]. \quad (9)$$

Substituting equations (9) into equations (1)–(4) (taking equation (8) into account) yields the following nonsimilar equations and boundary conditions:

$$\begin{aligned} \frac{1}{\varepsilon} f''' + \frac{1}{\varepsilon^2} \left( 1 + \frac{\xi \cos \xi}{\sin \xi} \right) f f'' + \frac{\sin \xi}{\xi} \theta - \left( Ha^2 + \frac{150(1-\varepsilon)^2}{\varepsilon^3 Da^2} \right) f' \\ - \frac{1}{\varepsilon^2} \left( 1 + \frac{1.75(1-\varepsilon)}{\varepsilon} \xi \Gamma \right) (f')^2 = \frac{\xi}{\varepsilon^2} \left( f' \frac{\partial f'}{\partial \xi} - f'' \frac{\partial f}{\partial \xi} \right), \end{aligned} \quad (10)$$

$$\frac{1}{Pr} \theta'' + Ds(f' \theta')' + \left( 1 + \frac{\xi \cos \xi}{\sin \xi} \right) f \theta' = \xi \left( f' \frac{\partial \theta}{\partial \xi} - \theta' \frac{\partial f}{\partial \xi} \right). \quad (11)$$

The boundary conditions are defined as follows:

$$\begin{aligned} \eta = 0: \quad f' = 0, \quad \xi \frac{\partial f}{\partial \xi} + \left( 1 + \frac{\xi \cos \xi}{\sin \xi} \right) f = f_w, \quad \theta' = -1, \\ \eta \rightarrow \infty: \quad f' = 0, \quad \theta = 0, \end{aligned} \quad (12)$$

where

$$\begin{aligned} Ha^2 = \frac{\sigma B_0^2 a^2}{\rho \nu (Gr)^{2/5}}, \quad Da = \frac{d(Gr)^{1/5}}{a}, \quad \Gamma = a/d, \\ Ds = \frac{\gamma d (Gr)^{2/5}}{a}, \quad Pr = \frac{\nu}{\alpha}, \quad f_w = -\frac{V_w a}{\nu (Gr)^{1/5}}, \end{aligned} \quad (13)$$

are the square of the Hartmann number, the Darcy number, the Forchheimer number, dispersion parameter, the Prandtl number and the suction/injection parameter, respectively.  $f_w < 0$  for  $V_w > 0$  (the case of injection), and  $f_w > 0$  for  $V_w < 0$  (the case of suction). The transformed form of the variable porosity function becomes

$$\varepsilon(\eta) = \varepsilon_\infty (1 + b \exp(-c\eta/Da)) \quad (14)$$

At  $x = 0$ , the following similarity equations and boundary conditions are obtained:

$$\frac{1}{\varepsilon} f''' + \frac{1}{\varepsilon^2} (2f f'' - (f')^2) + \theta - \left( Ha^2 + \frac{150(1-\varepsilon)^2}{\varepsilon^3 Da^2} \right) f' = 0, \quad (15)$$

$$\frac{1}{Pr} \theta'' + Ds(f' \theta')' + 2f \theta' = 0, \quad (16)$$

$$\begin{aligned} \eta = 0: \quad f' = 0, \quad f = \frac{f_w}{2}, \quad \theta' = -1, \\ \eta \rightarrow \infty: \quad f' = 0, \quad \theta = 0. \end{aligned} \quad (17)$$

The physical quantities of interests are the skin-friction coefficient (wall shear stress) and the Nusselt number, which can be expressed as:

$$C_{fx} = \frac{\tau_w}{\rho(\nu/a)^2(Gr)^{3/5}} = \xi f''(\xi, 0), \tag{18}$$

$$Nu = \frac{ha}{k_e} = (Gr)^{1/5} \frac{1}{\theta(\xi, 0)}, \quad \text{or} \quad Nu(Gr)^{-1/5} = \frac{1}{\theta(\xi, 0)}. \tag{19}$$

### 3 Numerical method

We now discuss the local nonsimilarity method to solve equations (10) and (11). Since it was already seen in papers of Minkowycz and Sparrow [25,26] that for the problem of coupled local nonsimilarity equations, consideration of equation up to the second level of truncation gives almost accurate results comparable with the solutions from other methods such as finite difference method, we will consider here the local nonsimilar equations (10) and (11) only up to the second level of truncation. To do this, we introduce the following new functions:  $G = \partial f / \partial \xi$  and  $\varphi = \partial \theta / \partial \xi$ . Introducing these functions into (10)–(12) we get

$$\begin{aligned} \frac{1}{\varepsilon} f''' + \frac{1}{\varepsilon^2} \left( 1 + \frac{\xi \cos \xi}{\sin \xi} \right) f f'' + \frac{\sin \xi}{\xi} \theta - \left( Ha^2 + \frac{150(1-\varepsilon)^2}{\varepsilon^3 Da^2} \right) f' \\ - \frac{1}{\varepsilon^2} \left( 1 + \frac{1.75(1-\varepsilon)}{\varepsilon} \xi \Gamma \right) (f')^2 = \frac{\xi}{\varepsilon^2} (f' G' - f'' G), \end{aligned} \tag{20}$$

$$\frac{1}{Pr} \theta'' + Ds(f' \theta')' + \left( 1 + \frac{\xi \cos \xi}{\sin \xi} \right) f \theta' = \xi (f' \varphi - \theta' G). \tag{21}$$

Differentiating the above equations with respect to  $\xi$  one may easily find by neglecting the terms involving the derivative functions of  $G$  and  $\varphi$  with respect to  $\xi$  as follows:

$$\begin{aligned} \frac{1}{\varepsilon} G''' + \frac{1}{\varepsilon^2} \left( 1 + \frac{\xi \cos \xi}{\sin \xi} \right) (f G'' + G f'') + \frac{1}{\varepsilon^2} \left( \frac{\cos \xi}{\sin \xi} - \frac{\xi}{\sin^2 \xi} \right) f f'' \\ + \frac{\sin \xi}{\xi} \varphi + \frac{1}{\xi^2} (\xi \cos \xi - \sin \xi) \theta - \left( Ha^2 + \frac{1.50(1-\varepsilon)^2}{\varepsilon^3 Da^2} \right) G' \\ - \frac{1}{\varepsilon^2} \left( 1 + \frac{1.75(1-\varepsilon)}{\varepsilon} \xi \Gamma \right) 2f' G' - \left( \frac{1.75(1-\varepsilon)}{\varepsilon^3} \Gamma \right) (f')^2 \\ = \frac{\xi}{\varepsilon^2} ((G')^2 - G G'') + \frac{1}{\varepsilon^2} (f' G' - f'' G), \end{aligned} \tag{22}$$

$$\begin{aligned} \frac{1}{Pr} \varphi'' + Ds(f' \varphi' + G' \theta')' + \left( 1 + \frac{\xi \cos \xi}{\sin \xi} \right) (f \varphi' + G \theta') \\ + \left( \frac{\cos \xi}{\sin \xi} - \frac{\xi}{\sin^2 \xi} \right) f \theta' = \xi (G' \varphi - G \varphi') + f' \varphi - \theta' G. \end{aligned} \tag{23}$$

The appropriate boundary conditions to be satisfied by the above equations are

$$\begin{aligned}
 \eta = 0: \quad & f' = G' = \varphi' = 0, \quad \theta' = -1, \quad \xi G + \left(1 + \frac{\xi \cos \xi}{\sin \xi}\right) f = f_w, \\
 & \left(2 + \frac{\xi(\sin \xi + \cos \xi)}{\sin \xi}\right) G + \left(\frac{\cos \xi}{\sin \xi} - \frac{\xi}{\sin^2 \xi}\right) f = 0, \\
 \eta \rightarrow \infty: \quad & f' = G' = 0, \quad \theta = \varphi = 0.
 \end{aligned} \tag{24}$$

### 4 Results and discussions

The numerical results for the dimensionless velocity and temperature, as well as the local skin friction coefficient and the Nusselt number are obtained for representative values of the dimensionless coordinate  $\xi$ , the Forchheimer number  $\Gamma$ , the Hartmann number  $Ha$ , the Darcy number  $Da$ , the Prandtl number  $Pr$ , dispersion parameter  $Ds$  and the suction/injection parameter  $f_w$ . The system of the governing equations (10)–(11) together with the boundary conditions (12) is nonlinear partial differential equations are integrated by the local nonsimilarity method for flow with a variable porosity media. The present results are validated with previously published work. We have compared our numerical results those of Huang and Chen [7], Chiang et al. [6], Lien et al. [8], and Yih [9] in the absence of magnetic field, porosity, Darcy number, inertia resistance and thermal dispersion effects. The comparisons are found to in good agreement, as shown in Tables 1, 2. The  $\eta$  values were chosen so that the outer boundary  $\eta_e = 10$ , which is sufficiently large, and they are such that the grid is sufficiently dense in the vicinity of the boundary to ensure accuracy; this is important because the boundary layer thins substantially as  $\xi$  increases. It should be noted that, the differences in  $\theta(\xi, 0)$  and  $f''(\xi, 0)$  at some  $\xi$  appear in Tables 1, 2 is due to using small  $\eta$  than those mentioned with numerical results of the above references such that  $f'(\xi, \eta)$  and  $\theta(\xi, \eta)$  profiles go asymptotically to zero.

Table 1. Comparison of  $f''(\xi, 0)$  for various values of  $Pr$  with uniform porosity (i.e.,  $b = 0, \varepsilon_\infty = 1.0, Da = \infty, Ha = 0, Ds = 0.0, \Gamma = 0.0$  and  $f_w = 0.0$ )

$Pr$	$\xi$	Huang and		Chamkha and	Present
		Chen [7]	Yih [9]	Al-Mudhaf [10]	
0.7	0°	1.2276	1.2278	1.2273	1.2278
	30°	1.2031	1.2032	1.2023	1.1985
	60°	1.1296	1.1297	1.1288	1.1038
	90°	1.0071	1.0072	1.0065	0.9204
7.0	0°	0.5165	0.5159	0.5157	0.5160
	30°	0.5065	0.5059	0.5058	0.5040
	60°	0.4768	0.4762	0.4761	0.4644
	90°	0.4276	0.4271	0.4271	0.3848

Table 2. Comparison of  $\theta(\xi, 0)$  for various values of  $Pr$  with uniform porosity (i.e.,  $b = 0, \varepsilon_\infty = 1.0, Da = \infty, Ha = 0, Ds = 0.0, \Gamma = 0.0$  and  $f_w = 0.0$ )

$Pr$	$\xi$	Chiang et al. [6]	Lien et al. [8]	Huang and Chen [7]	Yil [7]	Chamkha and Al-Mudhaf [10]	Present results
0.7	0°	1.8691	1.8700	1.8700	1.8689	1.8683	1.8691
	30°	1.8913	1.8931	1.8927	1.8917	1.8902	1.8867
	60°	1.9582	1.9653	1.9648	1.9638	1.9628	1.9336
	90°	2.0696	2.1026	2.1018	2.1004	2.0989	1.9811
7.0	0°	—	—	1.0350	1.0354	1.0341	1.0348
	30°	—	—	1.0477	1.0481	1.0471	1.0448
	60°	—	—	1.0879	1.0884	1.0872	1.0714
	90°	—	—	1.1642	1.1649	1.1636	1.0999

Fig. 2 illustrates the effects of imposing a magnetic field and Darcy number and increasing its strength on the velocity and temperature profiles at  $\xi = 30^\circ$ , respectively. The reference parametric conditions for which these and all subsequent figures are obtained correspond to two electrically conducting fluids, metal ammonia suspensions ( $Pr = 0.78$ ) and mercury ( $Pr = 0.027$ ) polluted in a variable porosity porous medium around the sphere in the presence of a magnetic field, permeability, the inertia and thermal dispersion effects. The imposition of a magnetic field normal to the flow direction produces a resistive force that decelerates the motion of the fluid in the porous medium and around the sphere with a resultant increase in the fluid temperature. These behaviors are depicted in Fig. 2 the influence of the magnetic Hartmann number  $Ha$  on the velocity  $f'(\xi, \eta)$  and temperature  $\theta(\xi, \eta)$  profiles, respectively. Application of a transverse magnetic field normal to the flow direction gives rise to the magnetic Lorentz force that acts in the opposite direction of flow causing its velocity to decrease and its temperature to increase. In addition, the thermal boundary layer tends to increase as  $Ha$  increases. Also, Fig. 2 depicted the influence of the Darcy number  $Da$  on the velocity and the temperature profiles, respectively. It is obvious that an increasing of  $Da$  increases the velocity distributions while decreases the temperature distribution. This means that the presence of porous medium causes higher restriction to the fluid, which reduces both the velocity and enhanced the temperature. In addition, slight increases in the boundary-layer thickness and decreases in the thermal boundary-layer thickness are observed as a result of increasing  $Da$ .

The variation of the skin friction coefficient  $C_{fx}$  and the local Nusselt number  $Nu(Gr)^{-1/5}$  with for various values of the Hatrmann number  $Ha$  and Darcy number  $Da$  is shown in Fig. 3. It can be seen that an increase of the Hatrmann number  $Ha$ , decreasing the Darcy number  $Da$  leads to decrease in the skin friction coefficient and the local Nusselt number. This may be attributed to the fact that represent additional resistance to flow, thus, slowing the fluid flow.

The effect of varying the effectives Prandtl number  $Pr$  corresponding to metal ammonia suspensions ( $Pr = 0.78$ ) and mercury ( $Pr = 0.027$ ), respectively and the suction

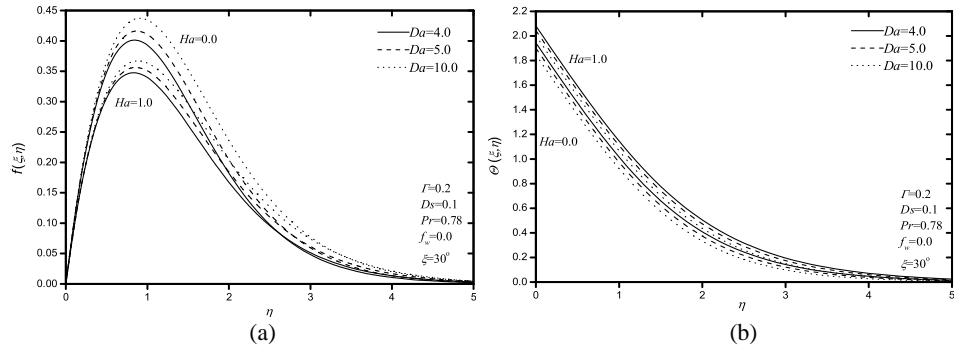


Fig. 2. Effects of  $Ha$  and  $Da$  on velocity profiles (a); on temperature profiles (b).

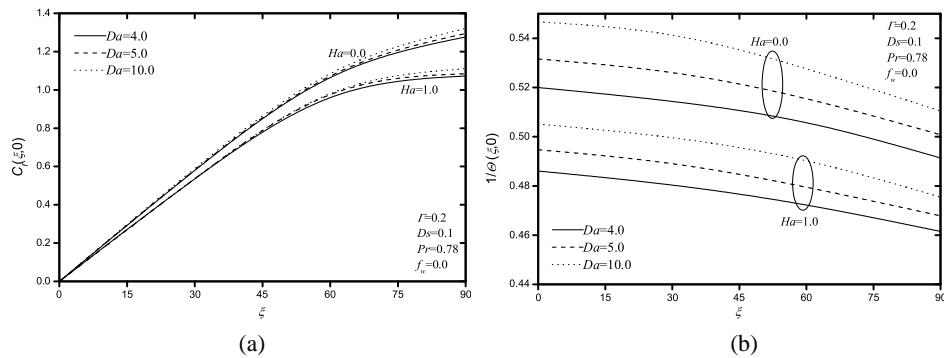


Fig. 3. Effects of  $Ha$  and  $Da$  on the skin friction coefficient (a); on local Nusselt number (b).

or injection parameter  $f_w$  on the on the velocity and temperature profiles is shown in Fig. 4. Increases in the values of  $Pr$  have a tendency to decrease both the fluid temperature and the thermal boundary-layer thickness. This causes a decrease in the thermal buoyancy effect which is causing the fluid flow. Therefore, both the fluid velocity and the hydrodynamic boundary-layer thickness decrease as  $Pr$  increases. Also, it can be seen, an imposition of wall fluid suction ( $f_w > 0$ ) tends to decelerate the flow around the sphere, with reduced temperature, whereas an imposition of fluid injection or blowing at the sphere surface ( $f_w < 0$ ) produces the opposite behavior, namely, an increase in the flow velocity and increases in the temperature.

In Fig. 5, the effects of  $f_w$  and  $Pr$  on the skin friction coefficient  $CP_{fx}$  and the local Nusselt number  $Nu(Gr)^{-1/5}$  are presented, respectively. In this figure, it is observed that, as  $Pr = 0.027$ , the skin friction coefficient  $C_{fx}$  increases, whereas the local Nusselt number  $Nu(Gr)^{-1/5}$  decreases as the suction/injection parameter  $f_w$  increases. But, as  $Pr = 0.78$ , both  $C_{fx}$ ,  $Nu(Gr)^{-1/5}$  increases as  $f_w$  increases, that is because from Fig. 5(a), where it is clearly seen that for  $Pr = 0.027$ , the wall slopes of the velocity profiles become steep and slightly increased as  $f_w$  increases, while they are clearly reduced

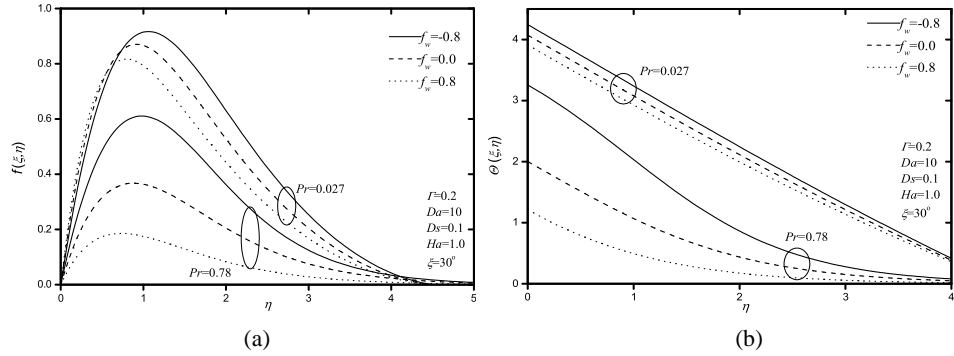


Fig. 4. Effects of  $f_w$  and  $Pr$  on velocity profiles (a); on temperature profiles (b).

for  $Pr = 0.78$ . The effect of enhancing the value of  $Pr$  is observed to decrease the values of  $C_{fx}$  and to increase the values of  $Nu(Gr)^{-1/5}$ .

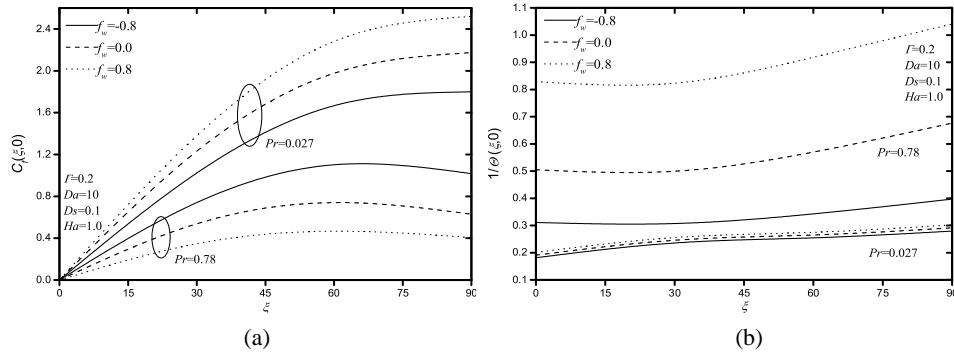


Fig. 5. Effects of  $f_w$  and  $Pr$  on velocity profiles (a); on temperature profiles (b).

Fig. 6 shows the influences of both the dispersion parameter  $Ds$  and Forchheimer number  $\Gamma$  on the both the velocity and temperature profiles. An observation of equation (8) shows that Forchheimer number  $\Gamma$  acts as the porous medium inertia effect which represents additional resistive force. Thus, increasing its value represents an increase in the resistance to the flow around the sphere. Thus, the fluid velocity decreases while its temperature increases as Forchheimer number  $\Gamma$  increases. But, the opposite behavior, as dispersion parameter  $Ds$  increases.

Finally, Fig. 7 depicts the variations in the skin friction coefficient  $C_{fx}$  and the local Nusselt number  $Nu(Gr)^{-1/5}$  that are brought about by simultaneous changes in the values of both the dispersion parameter  $Ds$  and Forchheimer number  $\Gamma$ , respectively. It is clear that, an increase of the dispersion values of  $Ds$ , decreases the skin friction coefficient, whereas, increases the Nusselt number. On other hand, increases in the values of  $\Gamma$  result in decreases in both the skin friction coefficient and Nusselt number. The

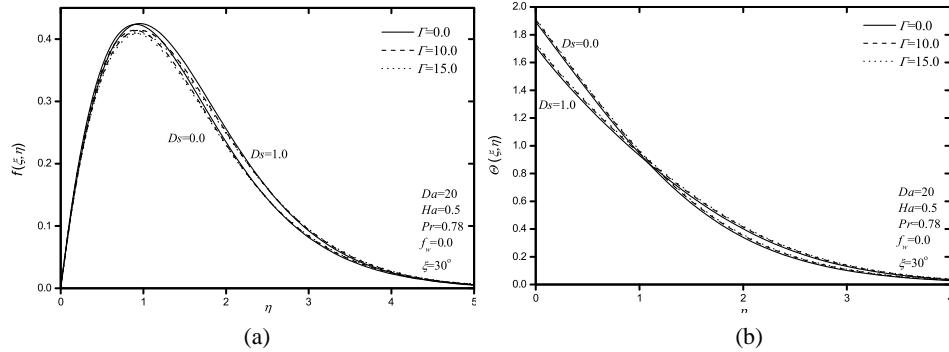


Fig. 6. Effects of  $\Gamma$  and  $D_s$  on velocity profiles (a); on temperature profiles (b).

decrease in the Nusselt number results from the increases in the temperature attained in the flow adjacent to the sphere surface, moreover, the resistance mechanism introduced by the inertia effects of the porous medium overcomes all other effects including the thermal buoyancy effect.

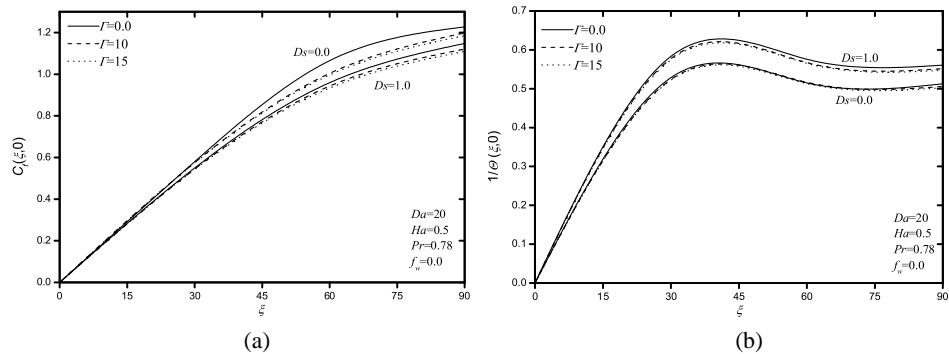


Fig. 7. Effects of  $\Gamma$  and  $D_s$  on the skin friction coefficient (a); on local Nusselt number (b).

## 5 Conclusions

The effect of thermal dispersion with the natural convection laminar boundary layer flow of an electric conducting fluid over a permeable sphere embedded in a variable porosity porous medium using the Brinkman-Forchheimer-Darcy extended model. The surface of sphere was maintained at uniform heat flux and permeable so as to allow for fluid wall suction or injection. Local nonsimilarity scheme has been used to solve numerically the transformed governing equations. Calculations were carried out for a wide range of values of the pertinent parameters to examine the results from this method. Graphical results for the velocity and temperature profiles as well as the skin friction coefficient

and Nusselt number are presented and discussed for various parametric conditions. It has been found that the skin friction coefficient reduced due to increases in either the Forchheimer number, the Hartmann number, Prandtl number, the dispersion parameter and the suction/injection parameter for metal ammonia case, whereas the opposite behavior was predicted as the Darcy number and the suction/injection parameter for mercury case. Also, increasing in the values of the Darcy number, the Prandtl number, the dispersion parameter or the suction/injection parameter produced enhances in the local Nusselt number, and it was reduced due to increase in either the Forchheimer number or Hartmann number.

### Acknowledgments

The authors are grateful to the referees for making useful comments for improving this article.

### References

1. T. Yuge, Experiments on Heat Transfer from Spheres Including Combined Natural and Forced Convection, *J. Heat Transfer*, **82**, pp. 214–220, 1960.
2. L. S. Klaychko, Heat Transfer between a Gas and a Spherical Surface with the Combined Action of Free and Forced Convection, *J. Heat Transfer*, **85**, pp. 355–357, 1963.
3. C. A. Hieber, B. Gebhart, Mixed Convection from a Sphere at Small Reynolds and Grashof Numbers, *J. Fluid Mech.*, **38**, pp. 137–159, 1969.
4. T. S. Chen, A. Mucoglu, Analysis of Mixed Forced and Free Convection about a Sphere, *Int. J. Heat Mass Transfer*, **20**, pp. 867–875, 1977.
5. T. S. Chen, A. Mucoglu, Mixed Convection about a Sphere with Uniform Surface Heat Flux, *J. Heat Transfer*, **100**, pp. 542–544, 1978.
6. T. Chiang, A. Ossin, C. L. Tien, Laminar Free Convection from a Sphere, *J. Heat Transfer*, **86**, pp. 537–542, 1964.
7. M. J. Huang, C. K. Chen, Laminar Free-Convection from a Sphere with Blowing and Suction, *J. Heat Transfer*, **109**, pp. 529–532, 1987.
8. F. S. Lien, C. K. Chen, J. W. Cleaver, Mixed and Free Convection over a Rotating Sphere with Blowing and Suction, *J. Heat Transfer*, **108**, pp. 398–404, 1986.
9. K. A. Yih, Viscous and Joule Heating Effects on Non-Darcy MHD Natural Convection Flow over a Permeable Sphere in Porous Media with Internal Heat Generation, *Int. Commun. Heat Mass Transfer*, **27**, pp. 591–600, 2000.
10. A. J. Chamkha, A. Al-Mudhaf, Simultaneous Heat And Mass Transfer From A Permeable Sphere At Uniform Heat And Mass Fluxes With Magnetic Field And Radiation Effects, *Num. Heat Transfer A*, **46**, pp. 181–198, 2004.

11. O. Plumb, The effect of thermal dispersion on heat transfer in packed bed boundary layers, in: *Proceedings of First ASME/JSME Thermal Engineering Joint Conference*, **2**, pp. 17–21, 1983.
12. J. T. Hong, Y. Yamada, C. L. Tien, Effects of non-Darcian and non-uniform porosity on vertical plate natural convection in porous media, *J. Heat Transfer*, **109**, pp. 356–361, 1987.
13. F. C. Lai, F. A. Kulacki, Thermal dispersion effects on non-Darcy convection over horizontal surfaces in saturated porous media, *Int. J. Heat Mass Transfer*, **32**, pp. 971–976, 1989.
14. F. C. Lal, F. A. Kulacki, Non-Darcy mixed convection along a vertical wall in saturated porous medium, *J. Heat Transfer*, **113**, pp. 252–255, 1991.
15. A. Amiri, K. Vafai, Analysis of dispersion effects and non-thermal equilibrium non-Darcian variable porosity incompressible flow through porous media, *Int. J. Heat Mass Transfer*, **37**, pp. 939–954, 1994.
16. J. T. Hong, C. L. Tien, Analysis of thermal dispersion effect on vertical plate natural convection in porous media, *Int. J. Heat Mass Transfer*, **30**, pp. 143–150, 1987.
17. P. V. S. N. Murthy, P. Singh, Thermal dispersion effects on non-Darcy natural convection with lateral mass flux, *Heat and Mass Transfer*, **33**, pp. 1–5, 1997.
18. P. V. S. N. Murthy, P. Singh, Thermal dispersion effects on non-Darcy convection over a cone, *Computers and Mathematics with Applications*, **40**, pp. 1433–1444, 2000.
19. K. Vafai, C. L. Tien, Boundary and inertia effects on flow and heat transfer in porous media, *Int. J. Heat Mass Transfer*, **24**, pp. 195–203, 1981.
20. B. Gebhart, Y. Jaluria, R. L. Mahajan, B. Sammakia, *Buoyancy-Induced Flows and Transport*, Hemisphere, New York, 1988.
21. D. Poulikakos, K. Renken, Forced convection in a channel filled with porous medium, including the effects of flow inertia, variable porosity, and Brinkman friction, *ASME J. Heat Transfer*, **109**, pp. 880–888, 1987.
22. K. Vafai, Heat transfer in variable porosity media, *J. Fluid Mech.*, **147**, pp. 233–259, 1984.
23. K. Vafai, R. L. Alkire, C. L. Tien, An experimental investigation of heat transfer in variable porosity media, *ASME J. Heat Transfer*, **107**, pp. 642–647, 1985.
24. R. F. Benenati, C. B. Brosilow, Void fraction distribution in packed beds, *AIChE J.*, **8**, pp. 359–361, 1962.
25. W. J. Minkowycz, E. M. Sparrow, Numerical solution scheme for local nonsimilarity boundary-layer analysis, *Numer. Heat Transfer*, **1**, pp. 69–85, 1978.
26. W. J. Minkowycz, E. M. Sparrow, Interaction between surface mass transfer and transverse curvature in natural convection boundary layers, *Int. J. Heat Mass Transfer*, **22**, pp. 1445–1454, 1979.